Geomechanics and Engineering, *Vol. 20, No. 6 (2020) 517-525*
DOI: https://doi.org/10.12989/gae.2020.20.6.517

Modeling time-dependent behavior of hard sandstone using the DEM method

Wen-Bin Guo*[1,2], Bo Hu**[1,3], Jian-Long Cheng[4] and Bei-Fang Wang[5]

[1]Inner Mongolia Key Laboratory of Mining Pressure and Strata Control, Hulunbeir University, Hulunbeir 021008, China
[2]College of Engineering and Technology, Hulunbeir University, Hulunbeir 021008, China
[3]State Key Laboratory for Geomechanics and Deep Underground Engineering, China University of Mining and Technology, Xuzhou 221116, China
[4]State Key Laboratory of Geohazard Prevention and Geoenvironment Protection, Chengdu University of Technology, Chengdu 610059, China
[5]State Key Laboratory of Water Resource Protection and Utilization in Coal Mining, Beijing 100011, China

(Received October 14, 2019, Revised February 8, 2020, Accepted February 17, 2020)

Abstract. The long-term stability of rock engineering is significantly affected by the time-dependent deformation behavior of rock, which is an important mechanical property of rock for engineering design. Although the hard rocks show small creep deformation, it cannot be ignored under high-stress condition during deep excavation. The inner mechanism of creep is complicated, therefore, it is necessary to investigate the relationship between microscopic creep mechanism and the macro creep behavior of rock. Microscopic numerical modeling of sandstone creep was performed in the investigation. A numerical sandstone sample was generated and Parallel Bond contact and Burger's contact model were assigned to the contacts between particles in DEM simulation. Sensitivity analysis of the microscopic creep parameters was conducted to explore how microscopic parameters affect the macroscopic creep deformation. The results show that the microscopic creep parameters have linear correlations with the corresponding macroscopic creep parameters, whereas the friction coefficient shows power function with peak strength and Young's modulus, respectively. Moreover, the microscopic parameters were calibrated. The creep modeling curve is in good agreement with the verification test result. Finally, the creep curves under one-step loading and multi-step loading were compared. This investigation can act as a helpful reference for modeling rock creep behavior from a microscopic mechanism perspective.

Keywords: hard sandstone; creep simulation; particle flow code; parallel bond model; Burger's model

1. Introduction

The elastic and plastic deformations are two important mechanical properties of rock. However, the time-dependent deformation and strength deterioration become more and more pronounced under deep excavations (Malan 2002, Wu and Shao 2019a,b). After excavation, the high in-situ stresses redistributed and the excavation closure increased gradually with increasing time. This phenomenon is related to rock creep. From the different failure scales view, the cracks accumulated from micro-scale size to macro-scale size represents the damage evolution within the intact rock. The final macro-failure of rock engineering is induced by the accumulated micro-failure (Miura *et al.* 2003, Li and Konietzky, 2014). Therefore, it is essential to investigate the creep behavior of rock, especially from the micro-scale size view. Further investigation on the creep deformation from the micro-scale will improve our understanding of the time-dependent failure of rock.

During the creep experiment, the rock sample is subjected to constant stress and deforms at a period time. The strain increases at a decreasing rate before tertiary creep until macro failure occurs. This time-dependent deformation is common to most of the rocks (Shin *et al.* 2005, Amitrano and Helmstetter 2006, Brantut *et al.* 2013, Sharifzadeh *et al.* 2013, Sone and Mark 2014, Wu *et al.* 2020). The creep failure is the result of micro-crack accumulation at which micro-crack propagates and reaches a critical threshold (Cai *et al.* 2004, Damjanac and Fairhurst 2010, Bikong *et al.* 2015). Atkinson (1984) reported that the mechanism of time-dependent deformation is subcritical crack growth also stress corrosion. Therefore, what is the relationship between the macroscopic phenomenon and micro-mechanism? This problem has attracted the attention of many researchers. Damage can indirectly indicate overall micro-crack growth. Various micro-mechanical-based models were built to describe rock creep deformation from the view of fracture and damage mechanics (Scholz 1968, Ashby 1990, Bhat *et al.* 2011). However, the creep equations are complicated, which is hard to apply.

Numerical simulation is an effective tool to reproduce the macroscopic creep deformation. Moghadam *et al.* (2013) presented an elasto-viscoplastic model to describe the short-term and long-term failure of rock salt and simulated the time-dependent deformation of an underground cavern. Mohanty and Vandergrift (2012) used a numerical simulation method to account for the time-

*Corresponding author, Professor
E-mail: guowenbin@hlbec.edu.cn
**Co-Corresponding author, Ph.D.
E-mail: huboskl@hotmail.com

http://www.techno-press.org/?journal=gae&subpage=7
ISSN: 2005-307X (Print), 2092-6219 (Online)

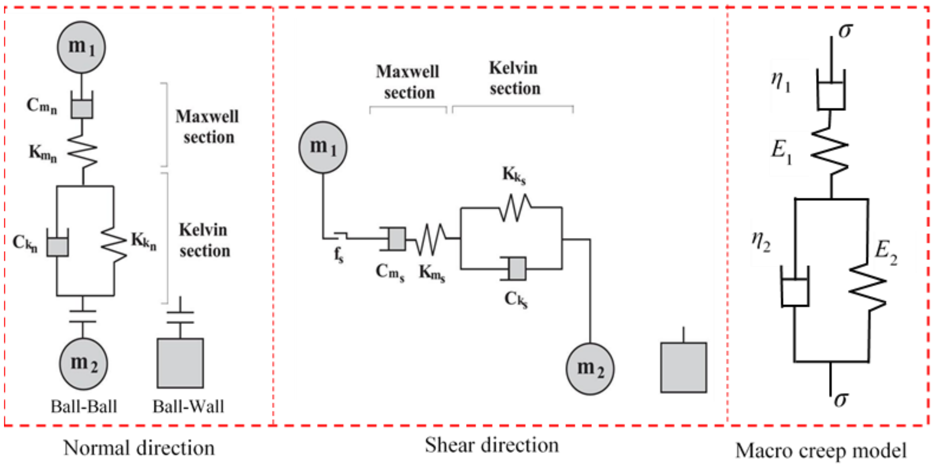

Fig. 1 Micro creep model in PFC and macro Burger's model (after Itasca 2004)

dependent deformation of a cavern serviced 30 years. Koyama and Jing (2007) used a REV concept model to simulate the micro-mechanical property of intact rock and also analyzed the influence of model size and particle size. Lajtai and Bielus (1986) reported that the time-dependent microcracking is the mechanism of rock subjected to creep loading. Chen and Konietzky (2014) developed a grain-based model to simulate the creep failure of the Lac du Bonnet granite by using the DEM model. Xue *et al.* (2017) utilized 3DEC to reproduce the time-dependent deformation of roof rock in coal mining. The discrete element method is better to characterize the macroscopic mechanical behavior of rock from the microscopic view, especially for the particle flow code (PFC) (Cundall and Strack 1979, Itasca 2004, Wang and Cai 2020). Potyondy (2007) developed a stress corrosion model to simulate the time-dependent cracking of rock based on the particle flow code method. Song *et al.* (2019) proposed a nonlinear stress corrosion model based on parallel-bonded model and simulated the time-dependent failure of the artificial rock. Numerical simulation can capture the development of micro-cracks during the creep stage. Bahrani *et al.* (2014) simulated the deformation and failure behaviors of the intact and granulated marble from the view of the grain-based model by using the PFC2D model. Li *et al.* (2017) used PFC2D to simulate the creep deformation of salt rock based on the installed contact model in the procedure. Gutiérrez-Ch *et al.* (2019) simulated the creep deformation of the slate rock using an implemented model in PFC2D and compared the simulation and test results. Liu and Cai (2018) utilized grain-based model in PFC to simulate the creep deformation and failure of brittle rock. Li *et al.* (2020) built a 3D grain-based rock salt specimen to reproduce its creep behavior in PFC.

However, the determination of the micro parameters in PFC is complicated and time-consuming. There are few investigations on the relationships between microscopic creep parameters in PFC and the macroscopic creep parameters of the rock sample. Therefore, this investigation aims to solve this problem and present a reference for calibration microscopic creep parameters in PFC based on the experimental creep curves.

2. Burger's contact model description in PFC2D

PFC2D is a kind of two dimensional DEM software that can simulate the rock mechanical behaviors by the acting between particles (Itasca 2004). In PFC procedure, there are several contact constitutive models to simulate different mechanical behaviors of materials, such as Contact-Bond model, Parallel-Bond model, Hysteretic Damping models, etc. Burger's model is widely used to describe the rheological deformation of a material. In PFC2D modeling procedure, the creep mechanism of the material is realized by the implemented Burger's contact between particles. Burger's contact model is composed of a Kelvin model and a Maxwell model in series, as shown in Fig. 1. Burger's model is installed in both normal and shear directions of the contact. The micro creep parameters in normal direction include the stiffness of linear springs (e.g., K_{mn} and K_{kn}) and the viscosity of dashpots (e.g., C_{mn} and C_{kn}). Similarly, K_{ms}, K_{ks}, C_{ms} and C_{ks} are the micro parameters in the shear direction. In addition, a slider component with friction f_s is in series with Burger's model for limiting the shear force acting at the contact between two particles.

In normal and shear directions, the displacement (u) of Burger's model can be decomposed of two sections, including Maxwell section (u_m) and Kelvin section (u_k). For the Maxwell model, the deformation includes linear spring (u_{mk}) displacement and dashpot displacement (u_{mc}). As a result, the total displacement is expressed as (Itasca 2004):

$$u = u_m + u_k = u_{mk} + u_{mc} + u_k \tag{1}$$

The first and second derivatives of the above equation can be expressed as:

$$\dot{u} = \dot{u}_{mk} + \dot{u}_{mc} + \dot{u}_k \tag{2}$$

$$\ddot{u} = \ddot{u}_{mk} + \ddot{u}_{mc} + \ddot{u}_k \tag{3}$$

The contact force ("+", "-" denotes normal and shear direction, respectively) and its first derivative in Kelvin section is expressed as

$$\begin{aligned} f &= \pm K_k u_k \pm C_k \dot{u}_k \\ \dot{f} &= \pm K_k \dot{u}_k \pm C_k \ddot{u}_k \end{aligned} \tag{4}$$

Similarly, the contact force and its first and second derivatives in Maxwell section are:

$$\begin{cases} f = \pm K_m u_{mk} \\ \dot{f} = \pm K_m \dot{u}_{mk} \\ \ddot{f} = \pm K_m \ddot{u}_{mk} \end{cases} \quad \begin{cases} f = \pm C_m \dot{u}_{mc} \\ \dot{f} = \pm C_m \ddot{u}_{mc} \end{cases} \tag{5}$$

Based on the Eqs. (2) to (5), the relationship between force and displacement is:

$$f + \left[\frac{C_k}{K_k} + C_m\left(\frac{1}{K_k} + \frac{1}{K_m}\right)\right]\dot{f} + \frac{C_k C_m}{K_k K_m}\ddot{f} = \pm C_m \dot{u} \pm \frac{C_k C_m}{K_k}\ddot{u} \tag{6}$$

Based on Eq. (4), the first derivative of the displacement in Kelvin section is:

$$\dot{u}_k = \frac{-K_k u_k \pm f}{C_k} \tag{7}$$

By using the central difference format described below, the force of a given step can be updated based on the force value of the previous step, the displacement values of the current and the previous steps. The average values for u_k and f are used.

$$\frac{u_k^{t+1} - u_k^t}{\Delta t} = \frac{1}{C_k}\left[-\frac{K_k(u_k^{t+1} + u_k^t)}{2} \pm \frac{f^{t+1}}{f^t}\right] \tag{8}$$

Therefore,

$$u_k^{t+1} = \frac{1}{a}\left[b u_k^t \pm \frac{\Delta t}{2C_k}(f^{t+1} + f^t)\right] \tag{9}$$

$$a = 1 + \frac{K_k \Delta t}{2C_k}, b = 1 - \frac{K_k \Delta t}{2C_k} \tag{10}$$

For Maxwell section:

$$\frac{u_m^{t+1} - u_m^t}{\Delta t} = \pm\frac{f^{t+1} - f^t}{K_m \Delta t} \pm \frac{f^{t+1} + f^t}{2C_m} \tag{11}$$

Therefore,

$$u_m^{t+1} = \pm\frac{f^{t+1} - f^t}{K_m} \pm \frac{\Delta t(f^{t+1} + f^t)}{2C_m} + u_m^t \tag{12}$$

The total displacement and its first derivate are:

$$\begin{aligned} u &= u_m + u_k \\ \dot{u} &= \dot{u}_m + \dot{u}_k \end{aligned} \tag{13}$$

The first-order difference format for time derivation is:

$$u^{t+1} - u^t = u_m^{t+1} - u_m^t + u_k^{t+1} - u_k^t \tag{14}$$

Substituting Eqs. (11) and (12) to the above equation，the contact force is:

$$f^{t+1} = \pm\frac{1}{c}\left[u^{t+1} - u^t + \left(1 - \frac{b}{a}\right)u_k^t \mp d f^t\right] \tag{15}$$

where,

$$c = \frac{\Delta t}{2C_k a} + \frac{1}{K_m} + \frac{\Delta t}{2C_m}, d = \frac{\Delta t}{2C_k a} - \frac{1}{K_m} + \frac{\Delta t}{2C_m} \tag{16}$$

The new contact force f^{t+1} can be obtained from the results of u^{t+1}, u^t, u_k^t, f^t.

For macroscopic Burger's model (shown in Fig. 1), the creep constitutive equation in one-dimensional format is written as:

$$\varepsilon = \frac{\sigma}{E_1} + \frac{\sigma}{\eta_1}t + \frac{\sigma}{E_2}\left(1 - \exp(-\frac{E_2}{\eta_2}t)\right) \tag{17}$$

3. Calibration of the creep model

3.1 Numerical sample construction

The geometry of the numerical sample is approximately set as 50 mm in width and 100 mm in height based on the researched sample in creep test. The numerical sample consists of 2879 balls with a radius ranging from 0.5 to 0.83 mm. The density of the sample is set as 2400 kg·m^{-3}. Parallel Bond (PB) contact model is widely used to simulate the mechanical behaviors of rock and concrete materials (Itasca 2004, Cho *et al.* 2007). Therefore, PB model is installed between particles to simulate the strength property of the sandstone. However, this model cannot reflect the time-dependent deformation. As mentioned above, Burger's contact can describe the creep behavior of rock. In PFC2D 3.1 version, Burger's model is enclosed in the package which can be loaded using the "config cppudm" and "model load burwrv.dll" command. Fig. 2 illustrates the modeling sample and two kinds of contacts.

3.2 Sensitivity analysis of micro parameters

There are number of micro parameters of PB and Burger's contact constitutive models. It is important to determine the micro parameters reflecting the macro mechanical behavior of the sandstone. This investigation aims to validate the micro creep parameters and simulates

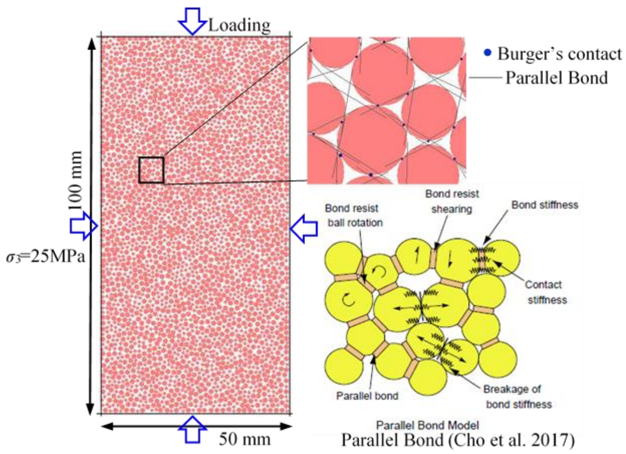

Fig. 2 Rock sample in numerical simulation

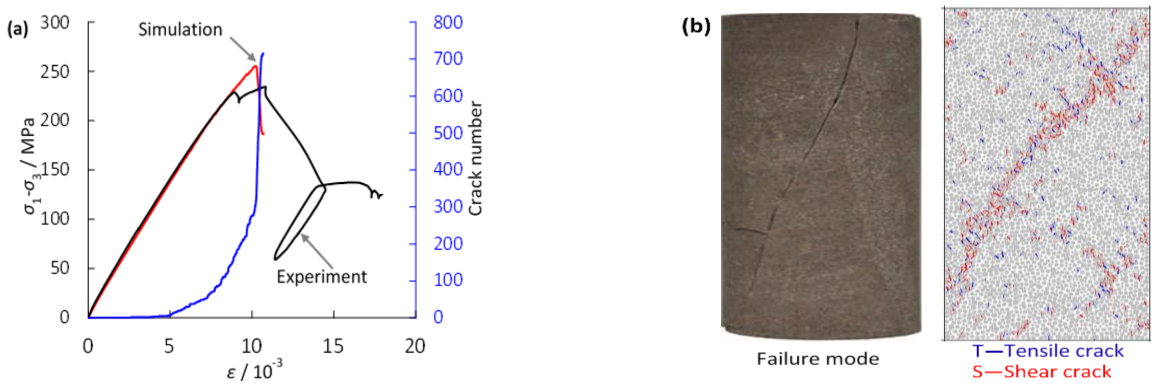

Fig. 3 Comparison results of the conventional triaxial compression in test and numerical simulation

Table 1 Microscopic parameters in PFC2D

Micro parameters of PB contact model	Values
Minimum ball radius /mm	0.5
Ratio of Max. ball radius to Min. ball radius	1.66
Sample density /kg·m^{-3}	2400
Elastic modulus of the ball /GPa	18.5
The stiffness ratio of the ball in normal and shear direction	1.5
Ball friction coefficient	0.6
The stiffness ratio of the PB contact in normal and shear direction	1.5
Elastic modulus of the PB contact /GPa	18.5
PB contact strength ± stand deviation in normal direction /MPa	15.0±3.75
PB contact strength ± stand deviation in shear direction /MPa	15.0±3.75

Table 2 Results of the conventional triaxial compression in test and simulation

	Confinement/MPa	Peak stress/MPa	Young's modulus/GPa
Test results	25	234.32	26.13
Simulation results	25	255.38	27.26

the macro creep deformation. Due to the Burger's model cannot reflect the strength property of the sandstone, PB model is first used to validate the basic deformation and strength characteristics shown in the conventional triaxial compression test under 25 MPa confinement. The Young's modulus and peak strength of the sandstone is obtained by 'Trial and error' method. The micro parameters are listed in Table 1 and the comparing results of the stress-strain curves and failure modes in the test and simulation are presented in Fig. 3.

There are four macroscopic creep parameters of macroscopic Burger's model, whereas there are nine microscopic creep parameters of microscopic Burger's model in PFC2D. What is the relationship between the micro and macro creep parameters? To simulate the macro creep behavior of the sandstone, it is important to determine and calibrate the micro creep parameters. Therefore, the sensitivity analysis of the micro creep parameters is necessary. There are four and five micro parameters in the normal and shear directions at a contact, respectively. To simplify the analysis process, the value ratio of the micro creep parameters in normal direction to that in shear direction is set as 1 (e.g., K_{mn}/K_{ms}=1). As a result, there are four micro creep parameters and a friction coefficient to perform sensitive analysis.

First, numerical creep tests are performed changing each micro creep parameter under the same deviatoric stress level applied in the creep test and plot the creep curves. Subsequently calculating the macro creep parameters based on the modeling creep curves. Then, analyzing the relationships between micro creep parameters and macro creep parameters. Fig. 4 presents the modeling creep curves with different micro parameters. As shown in Fig. 4(a), the larger is the stiffness of the Maxwell model (K_{mn}), the smaller is the axial strain. In Fig. 4(b), a large viscosity of the Maxwell model (C_{mn}) will result in a low steady-state creep rate. Moreover, as the stiffness of the Kelvin model (K_{kn}) increases, the creep deformation decreases as presented in Fig. 4(c). In Fig. 4(d), the larger is the viscosity of the Kelvin model (C_{kn}), the longer is the time for entering the secondary creep stage. For the friction coefficient (f_s), a larger f_s induces to a higher peak deviatoric stress as illustrated in Fig. 4(e).

The relationships between the micro creep parameters and macro creep parameters are obtained from Fig. 4. In Fig. 5, the direct influence of the changing micro parameters on the main macro parameters is plotted. The macro creep parameters are calculated by the strain-time curves from the numerical calculations. As shown in Fig. 5(a), the macro creep parameter (E_1) is significantly affected by the spring stiffness of the micro Maxwell model showing a linear correlation. The micro creep parameter (the viscosity of the Maxwell model C_{mn}) has a good linear correlation with the macro creep parameter (η_1). E_1 and η_1 affect the instantaneous deformation when applying the deviatoric stress and the strain rate at the secondary creep stage, respectively. Moreover, the micro parameter K_{kn} and C_{kn} mainly affect the macro parameters of the macro Kelvin model (E_2) and (η_2), respectively. The K_{kn} and C_{kn} show a linear correlation with E_2 and η_2, respectively. The micro parameter f_s has an obvious influence on the stress-strain of the sample and the elastic modulus showing nonlinear power function relationship. Although the quantitative

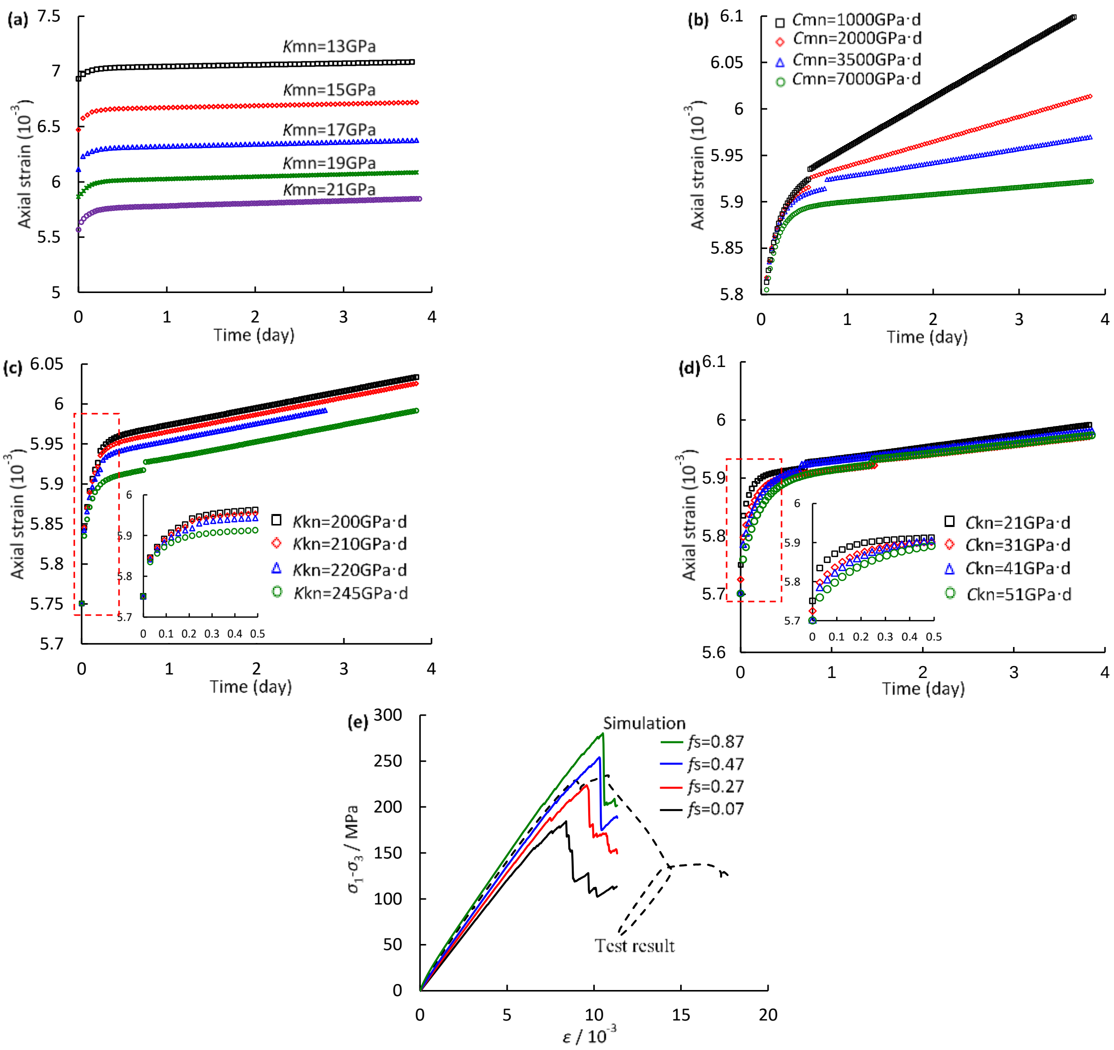

Fig. 4 Strain-time and stress-strain curves of the sample with different micro parameters

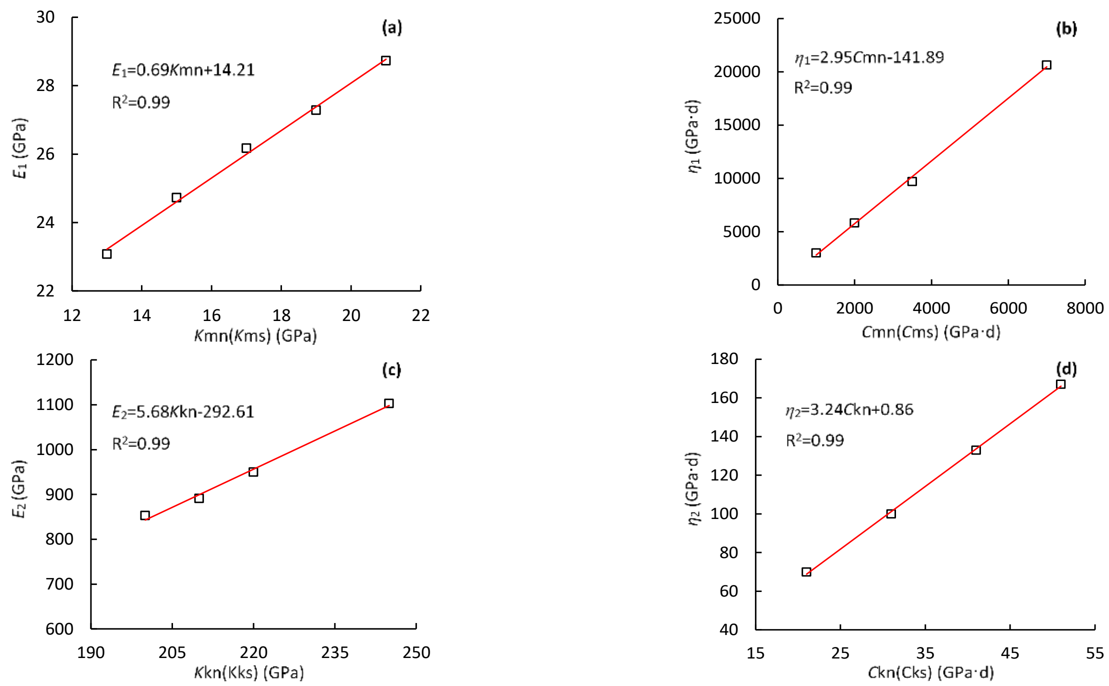

Fig. 5 Relationships between micro creep parameters and macro creep parameters

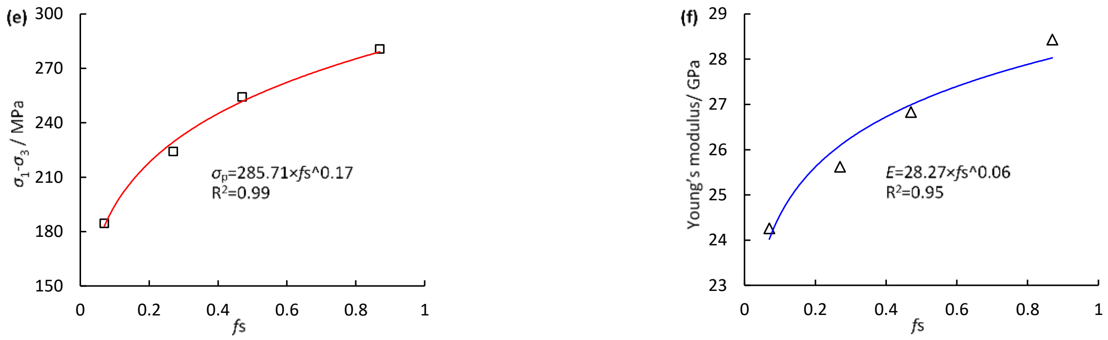

Fig. 5 Continued

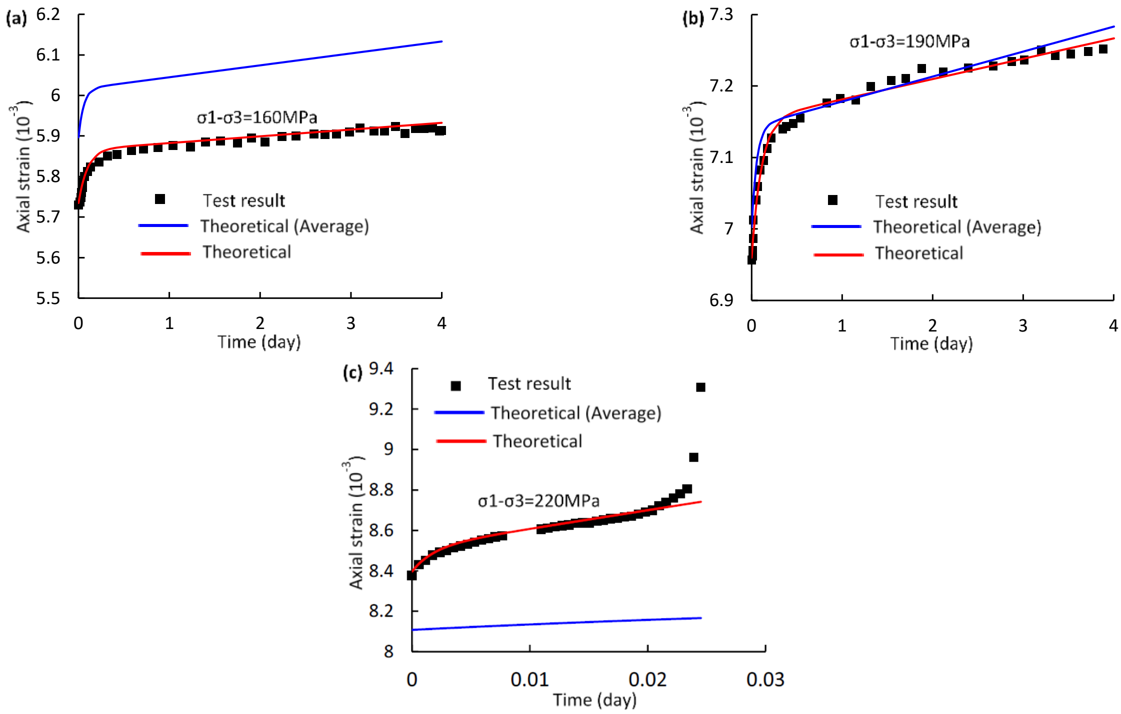

Fig. 6 Comparison results of the theoretical calculation and test results

Table 3 Macro creep parameters calculated by macro Burger's model

σ_1-σ_3/MPa	E_1/GPa	η_1/GPa·d	E_2/GPa	η_2/GPa·d
160	27.9	9613	1220	119
190	27.3	6679	984	106
220	26.2	23.95	1842	3.42
Average	27.18	5439	1349	76.14

relationships have been found, each micro parameter also has a minor impact on the other parameters. Therefore, the verification of the micro parameters should be minor adjusted based on the test results.

3.3 Validation with creep test of sandstone

The micro creep parameters are validated based on the creep test results. For the multi-step loading creep test on the sandstone, the confining pressure was 25 MPa and the applied deviatoric stresses were 160, 190 and 220 MPa. Each loading lasted for about 4 days until creep failure occurred. The one-dimensional macroscopic Burger's model is used to calculate the macro creep parameters. Fig. 6 and Table 3 present the fitting results. It should be noted that the red line represents the theoretical result based on each creep test under different deviatoric stress levels. Burger's model parameters are dependent on the stress level. The blue line represents the theoretical result calculated by the average values of each parameter. So the blue line doesn't agree well with the experimental curve except for the result at 190 MPa level. In addition, Burger's model cannot describe the tertiary creep, so the theoretical curve describes the decreasing creep and steady-state creep stage.

Subsequently, numerical validation is performed according to the test and theoretical calculation. Based on the relationships between micro and macro creep parameters obtained from the sensitivity analysis, the original numerical calculation is first conducted. If the numerical simulation curves do not agree well with the tested curves, the micro parameters should be adjusted

Table 4 Micro creep parameters of the micro Burger's model (σ_3=25 MPa)

K_{mn} (GPa)	K_{ms} (GPa)	C_{mn} (GPa·d)	C_{ms} (GPa·d)	K_{kn} (GPa)	K_{ks} (GPa)	C_{kn} (GPa·d)	C_{ks} (GPa·d)	f_s
19.3	19.3	3200/11.3	3200/11.3	245	245	35	35	0.47

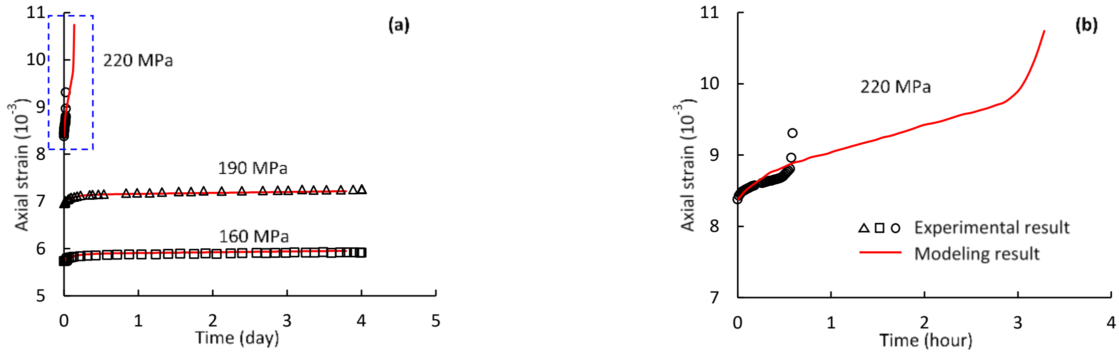

Fig. 7 Comparison of the numerical simulation and experimental result

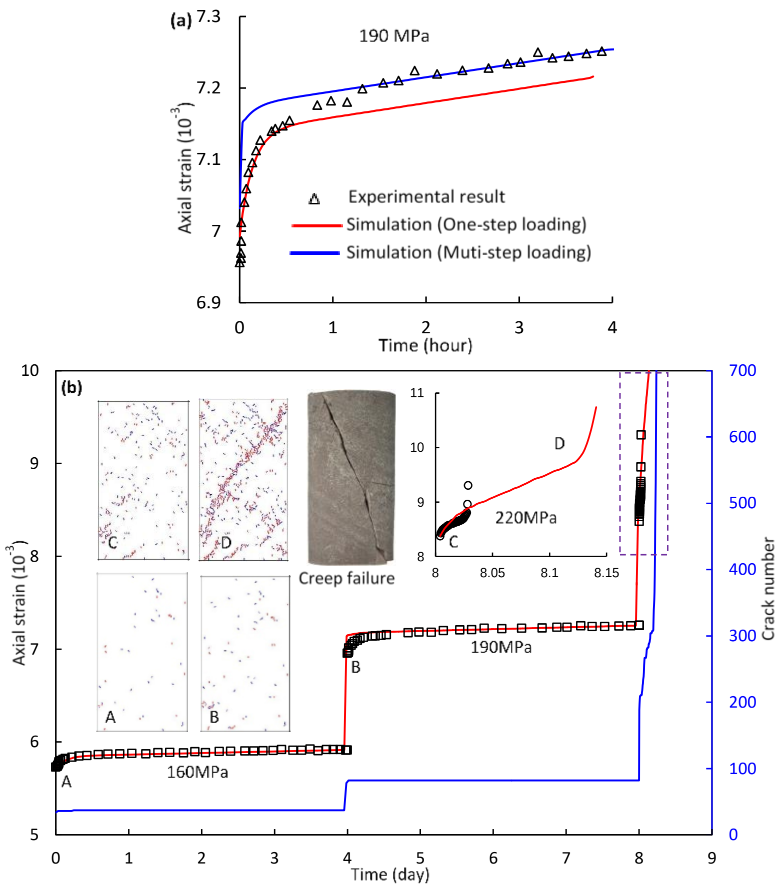

Fig. 8 Numerical simulation results of the sandstone under multi-step loading condition

appropriately until they agree well with the experiments. Table 4 lists the micro creep parameters used in numerical simulation. Fig. 7 presents the numerical simulation results and the experimental curves showing a good match. The simulation curves are obtained by one loading step. This means that 160,190 and 220MPa stress levels are applied to the numerical sample at three independent tests, respectively. Although Burger's model cannot simulate creep failure, PB model can reflect the strength of the sandstone. When the axial deformation reaches the limit value, failure will occur. So under 220 MPa deviatoric stress level, the axial strain increases gradually with the calculation step. Until it increases to the peak strain, creep failure will occur. However, during numerical simulation, the micro creep parameters are fixed, such as the viscosity of the micro Maxwell component (C_{mn}). So the strain rates at steady-state creep stages under different stress levels are similar. Under the creep failure stress level, the strain rate is larger more about two magnitudes than the other two stress levels. If the C_{mn} is still the same as that at 160 and 190 MPa, creep failure cannot appear. Therefore, this micro parameter is reduced from 3200 GPa·d to 11.3 GPa·d during the simulation at 220 MPa to simulate creep failure. The numerical simulation show later creep failure than the test result.

4. Discussion

For natural rock, there are more or less micro-pores or micro-cracks within the intact rock samples. Rock inhomogeneity significantly affects test results and their reliability. Different rock samples may show different laws. The multi-step loading creep method can avoid the influence of the rock difference.

The theoretical calculations are from each creep loading test, such as 160, 190 and 220 MPa, respectively. Therefore, the calculated macro parameters are affected by the loading history, especially for the 190 and 220MPa stress levels. In order to compare the influence of the loading history on the time-dependent deformation, one-step loading and multi-step loading are compared for the 190 MPa stress level creep. Fig. 8(a) presents the creep curves of the two loading methods and the test result where the red line denotes the one-step loading to 190 MPa and the blue one represents the 190MPa creep during a multi-step loading. It is clear that the multi-step loading method has a slightly larger deformation than that under one-step loading. The duration of the decreasing creep stage under one-step loading is more obvious than that under multi-step loading. Fig. 8(b) plots the creep curve of the numerical sample under a multi-step loading condition as well as the monitored crack numbers during the creep stage. The numerical calculation curve agrees well with the test data although the appearance of the creep failure is late under 220 MPa stress level comparing with the creep curve. During the loading stage, the increment of the crack number is more obvious than that during the constant loading stage. The crack distribution within the rock after applied the creep stresses and creep failure are plotted in Fig. 8(b) (e.g., A, B, C, and D). This also suggests that loading history also affects the creep deformation and crack accumulation during creep deformation and loading.

5. Conclusions

This investigation numerically studied the influence of the microscopic creep parameters in PFC2D on the macroscopic creep parameters of Burger's model, which is composed of a Maxwell body and a Kelvin component. Assuming the microscopic creep parameters in shear direction are the same as those in normal direction at a contact, some results are obtained as follows.

• The stiffness of Maxwell model (K_{mn}/K_{ms}) mainly affects the instantaneous deformation in a linear way. An increase in the viscosity of Maxwell model (C_{mn}/C_{ms}) will reduce the strain rate at the secondary creep stage.

• The larger is the stiffness of Kelvin model (K_{km}/K_{ks}), the smaller is the total creep deformation. A large value of the viscosity of Kelvin model (C_{kn}/C_{ks}) will increase the duration of decreasing creep stage.

• The microscopic creep parameters have linear correlations with the macroscopic creep parameters.

• The friction coefficient (f_s) makes the peak stress and Young's modulus change nonlinearly.

• The creep test was reproduced by the creep simulation, which agrees well with the test result. This investigation can increase our understanding of the macroscopic creep behavior of rock from the microscopic mechanism perspective.

Acknowledgments

This work is finically supported by the Open Fund of State Key Laboratory of Water Resource Protection and Utilization in Coal Mining (Grant No. SHJT-17-42.7), and Key Scientific Research Project of Inner Mongolia Universities (NJZZ20300).

References

Amitrano, D. and Helmstetter, A. (2006), "Brittle creep, damage, and time to failure in rocks", *J. Geophys. Res.*, **111**(B11), B11201. https://doi.org/10.1029/2005JB004252.

Ashby, M.F. and Sammis, C.G. (1990), "The damage mechanics of brittle solids in compression", *Pure Appl. Geophys.*, **133**(3), 489-521. https://doi.org/10.1007/BF00878002.

Atkinson, B.K. (1984), "Subcritical crack growth in geological materials", *J. Geophys. Res.*, **89**(B6), 4077-4114. https://doi.org/10.1029/JB089iB06p04077.

Bahrani, N., Kaiser, P.K. and Valley, B. (2014), "Distinct element method simulation of an analogue for a highly interlocked, non-persistently jointed rock mass", *Int. J. Rock Mech. Min. Sci.*, **71**,117-130. https://doi.org/10.1016/j.ijrmms.2014.07.005

Bhat, H.S., Sammis, C.G. and Rosakis, A.J. (2011), "The micromechanics of Westerly granite at large compressive loads", *Pure Appl. Geophys.*, **168**(12), 2181-2198. https://doi.org/10.1007/s00024-011-0271-9

Bikong, C., Hoxha, D. and Shao, J.F. (2015), "A micro-macro model for time-dependent behavior of clayey rocks due to anisotropic propagation of microcracks", *Int. J. Plasticity*, **69**, 73-88. https://doi.org/10.1016/j.ijplas.2015.02.001.

Brantut, N., Heap, M.J., Meredith, P.G. and Baud, P. (2013), "Time-dependent cracking and brittle creep in crustal rocks: A review", *J. Struct. Geol.*, **52**, 17-43. https://doi.org/10.1016/j.jsg.2013.03.007.

Cai, M., Kaiser, P.K., Tasaka, Y., Maejima, T., Morioka, H. and Minami, M. (2004), "Generalized crack initiation and crack damage stress thresholds of brittle rock masses near underground excavations", *Int. J. Rock Mech. Min. Sci.*, **41**(5), 833-847. https://doi.org/10.1016/j.ijrmms.2004. 02.001.

Chen, W. and Konietzky, H. (2014), "Simulation of heterogeneity, creep, damage and lifetime for loaded brittle rocks", *Tectonophysics*, **633**, 164-175. https://doi.org/10.1016/j.tecto.2014.06.033.

Cho, N., Martin, C.D. and Sego, D.C. (2007), "A clumped particle model for rock", *Int. J. Rock Mech. Min. Sci.*, **44**(7), 997-1010. https://doi.org/10.1016/j.ijrmms.2007.02.002.

Cundall, P.A. and Strack, O.D.L. (1979), "A discrete numerical model for granular assemblies", *Géotechnique*, **29**(1), 47-65. https://doi.org/10.1680/geot.1980.30.3.331.

Damjanac, B. and Fairhurst, C. (2010), "Evidence for a long-term strength threshold in crystalline rock", *Rock Mech. Rock Eng.*, **43**(5), 513-531. https://doi.org/10.1007/s00603-010-0090-9
Gutiérrez-Ch, J.G., Senent, S. and Jimenez, R. (2019), "Distinct Element Method Simulation of Creep Behaviour", *Proceedings of the 53rd US Rock Mechanics/Geomechanics Symposium*, New York, U.S.A. June.
Itasca Consulting Group Inc. (2004), *Particle Flow Code*, Itasca Consulting Group Inc., Sudbury, Canada.
Koyama, T. and Jing, L. (2007), "Effects of model scale and particle size on micro-mechanical properties and failure processes of rocks—a particle mechanics approach", *Eng. Anal. Bound. Elem.*, **31**(5), 458-472. https://doi.org/10.1016/j.enganabound.2006.11.009.
Lajtai, E.Z. and Bielus, LP. (1986), "Stress corrosion cracking of lac du bonnet granite in tension and compression", *Rock Mech. Rock Eng.*, **19**(2), 71-87. https://doi.org/10.1007/BF01042525.
Li, H., Yang, C.H., Ma, H.L., Shi, X.L., Zhang, H.N. and Dong, Z.K. (2020), "A 3D grain-based creep model (3D-GBCM) for simulating long-term mechanical characteristic of rock salt", *J. Petrol. Sci. Eng.*, **185**, 106672. https://doi.org/10.1016/j.petrol.2019.106672.
Li, W., Han, Y., Wang, T. and Ma, J. (2017), "DEM micromechanical modeling and laboratory experiment on creep behavior of salt rock", *J. Nat. Gas Sci. Eng.*, **46**, 38-46. https://doi.org/10.1016/j.jngse.2017.07.013
Li, X. and Konietzky, H. (2014), "Time to failure prediction scheme for rocks", *Rock Mech. Rock Eng.*, **47**(4), 1493-1503. https://doi.org/10.1007/s00603-013-0447-y.
Liu, G. and Cai, M. (2018), "Modeling time-dependent failure of brittle rock using PFC grain-based model", *Proceedings of the 52nd US Rock Mechanics/Geomechanics Symposium*, Seattle, Washington, U.S.A., June.
Malan, D.F. (2002), "Simulation of the time-dependent behavior of excavations in hard rock", *Rock Mech. Rock Eng.*, **35**(4), 225-254. https://doi.org/10.1007/s00603-002-0026-0.
Miura, K., Okui, Y. and Horii, H. (2003), "Micromechanics-based prediction of creep failure of hard rock for long-term safety of high-level radioactive waste disposal system", *Mech. Mater.*, **35**(3-6), 587-601. https://doi.org/10.1016/S0167-6636(02)00286-7.
Moghadam, N.S., Mirzabozorg, H. and Noorzad, A. (2013), "Modeling time-dependent behavior of gas caverns in rock salt considering creep, dilatancy and failure", *Tunn. Undergr. Sp. Technol.*, **33**, 171-185. https://doi.org/10.1016/j.tust.2012.10.001.
Mohanty, S. and Vandergrift, T. (2012), "Long term stability evaluation of an old underground gas storage cavern using unique numerical methods", *Tunn. Undergr. Sp. Technol.*, **30**, 145-154. https://doi.org/10.1016/j.tust.2012.02.015.
Potyondy, D.O. (2007), "Simulating stress corrosion with a bonded-particle model for rock", *Int. J. Rock Mech. Min. Sci.*, **44**(5), 677-691. https://doi.org/10.1016/j.ijrmms.2006.10.002.
Scholz, C.H. (1968), "The frequency-magnitude relation of micro fracturing in rock and its relation to earthquakes", *Bull. Seismol. Soc. Amer.*, **58**(1), 399-415.
Sharifzadeh, M., Tarifard, A. and Moridi, M.A. (2013), "Time-dependent behavior of tunnel lining in weak rock mass based on displacement back analysis method", *Tunn. Undergr. Sp. Technol.*, **38**, 348-356. https://doi.org/10.1016/j.tust.2013.07.014.
Shin, K., Okubo, S., Fukui, K. and Hashiba, K. (2005), "Variation in strength and creep life of six Japanese rocks", *Int. J. Rock Mech. Min. Sci.*, **42**(2), 251-260. https://doi.org/10.1016/j.ijrmms.2004.08.009.
Sone, H and Zoback, M.D. (2014), "Time-dependent deformation of shale gas reservoir rocks and its long-term effect on the in situ state of stress", *Int. J. Rock Mech. Min. Sci.*, **69**, 120-132. https://doi.org/10.1016/j.tust.2013.07.014.
Song, Z.Y., Konietzky, H. and Herbst, M. (2019), "Bonded-particle model-based simulation of artificial rock subjected to cyclic loading", *Acta Geotechnica*, **14**(4), 955-971. https://doi.org/10.1007/s11440-018-0723-9.
Wang, M.Z. and Cai, M. (2020), "A grain-based time-to-failure creep model for brittle rocks", *Comput. Geotech.*, **119**, 103344. https://doi.org/10.1016/j.compgeo.2019.103344.
Wu, K. and Shao, Z.S. (2019a), "Visco-elastic analysis on the effect of flexible layer on mechanical behavior of tunnels", *Int. J. Appl. Mech.*, **11**(3), 1950027. https://doi.org/10.1142/S1758825119500273.
Wu, K. and Shao, Z.S. (2019b), "Study on the effect of flexible layer on support structures of tunnel excavated in viscoelastic rocks", *J. Eng. Mech.*, **145**(10), 04019077. https://doi.org/10.1061/(ASCE)EM.1943-7889.0001657.
Wu, K., Shao, Z.S., Qin, S. and Li, B.X. (2020), "Determination of deformation mechanism and countermeasures in silty clay tunnel", *J. Perform. Constr. Fac.*, **34**(1), 04019095. https://doi.org/10.1061/(ASCE)CF.1943-5509.0001381.
Xue, Y.T, Mishra, B. and Gao, D. (2017), "Numerical and laboratory analysis of relaxation tests for determining time-dependent properties of rock", *Geotech. Geol. Eng.*, **35**(2), 615-629. https://doi.org/10.1007/s10706-016-0129-0.

GC